Calibration Procedure for an Inertial Measurement Unit Using a 6-Degree-of-Freedom Hexapod

Øyvind Magnussen, Morten Ottestad and Geir Hovland

***Abstract*— In this paper a calibration procedure for an Inertial Measurement Unit (IMU) mounted on an Unmanned Aerial Vehicle (UAV) is presented. Calibration of the sensor when it is mounted on the UAV is attractive because it combines calibration of the internal sensor parameters with the translational and rotational offsets of the IMU relative to the body frame of the UAV. A stepwise calibration procedure is presented, based on motion profiles and measurements generated by a 6-degree-of-freedom hexapod. The experimental results demonstrate that the linear acceleration and angular velocity measurements of the IMU sensor ADIS16400 can be calibrated to typically 0.17% and 0.25% of the ADIS16400 measurement range for linear acceleration and rotational velocity, respectively.**

I. INTRODUCTION

Unmanned aerial vehicles (UAVs) are often designed with an inherent instability and such systems can only be stabilized by feedback controllers using accurate sensors. In order to achieve high performance and robustness of such systems, it is essential that the sensor measurements are as accurate as possible. A typical sensor used in UAVs is an Inertial Measurement Unit (IMU) which measures linear accelerations and angular velocities in three dimensions. The IMU calibration is considered as one of the main challenges in inertial navigation. Even if highly accurate IMUs are available from sensor manufacturers it is still desirable to perform an independent calibration and verification of the performance against a more accurate measurement device. It is also desirable to calibrate the IMU after it has been mounted on the UAV, since the actual location and orientation of the sensor relative to the body frame of the UAV are additional error sources in the models and the feedback control algorithms. To ease the attitude calculations the IMU is often put in the center of gravity (CG) of the UAV with alignment of the sensor axes with the body frame. But UAVs, especially quadrotors, have limited space available and it can be difficult to place the IMU at the desired position.

In this paper an approach for calibration and verification of an IMU mounted on a UAV is presented. The approach uses the motion and sensing capabilities of a 6-degree-of-freedom (6-DOF) hexapod. By using a hexapod, it is possible to generate pure translational or rotational motion in selected directions, and this feature is exploited in a stepwise calibration procedure presented in this paper. Sensor parameters such as offsets, scaling factors, the alignment of the sensor's internal coordinate axes as well as the translational and rotational transformation relative to the UAV's body frame are identified.

The authors are with Faculty of Engineering and Science, Department of Engineering, University of Agder, Norway. E-mail of corresponding author: oyvind.magnussen@uia.no

Many authors have proposed different methods for IMU calibration, see [8] and the references therein. Common for these methods is the utilization of the fact that ideally the norm of the measured output of the accelerometer and gyro cluster is equal to the magnitude of the applied force and rotational velocity. As noted in [8] the main drawback of this approach is that not all the sensor parameters of the IMU are observable. This in turn implies that these uncalibrated parameters must be taken into account in the integration of the IMU in the UAV, for example with advanced filtering algorithms. There are also papers describing the process of calculating the new CG of the UAV if its shifted to a new location during operation [7]. Algorithms aligning two IMU in two reference frames has also been established [11]. But this does not count for misalignment of the internal axis-to-axis or scaling of the IMU. The research topic is not new, and old articles of how to automatically align an IMU relative to the earth [6] is also developed.

The main benefit of the work presented in this paper, is the flexibility of the hexapod to generate motions in selected directions. Hence, all the parameters of the IMU can be calibrated and the need for complex, online filtering techniques in the UAV real-time controller is reduced.

II. SYSTEM DESCRIPTION

A. Inertial Measurement Unit

An IMU, ADIS16400 from Analog Devices, measures acceleration a_I and angular velocity ω_I for the origin of the IMU frame for the three axes X_I, Y_I, Z_I as illustrated in Fig. 1. The subscripts I refer to the IMU's coordinate axes. In this paper, if the subscript does not begin with I, the variable is always referred to the body frame. In general, depending on how the IMU is mounted on the UAV, there will be rotations of the IMU's coordinate axes relative to the body axes (ϕ_I, θ_I, ψ_I), illustrated in Fig. 1.

In Fig. 2 the origin of the body frame is located at CG of the UAV. This is also the center of rotation for any rotational motion. The IMU frame is located off-center.

A off-center rotation of the IMU relative to the body frame, as in Fig 3, will result in additional accelerations perpendicular to the rotational axis, i.e. a radial acceleration a_R and a tangential acceleration a_T.

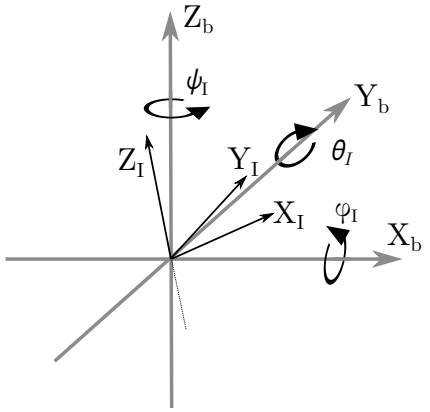

Fig. 1. *IMU frame relative to the body frame*

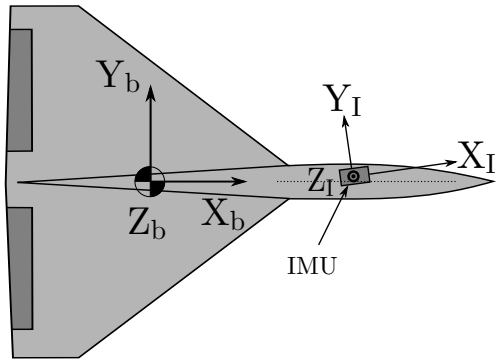

Fig. 2. *Rotation and translation of IMU frame relative to body frame.*

These accelerations specified in the body frame are described by [1] and [10]:

$$a_R = \omega_b \times (\omega_b \times R) \quad (1)$$

$$a_T = \alpha_b \times R \quad (2)$$

where $\times$ is the vector cross product, $R = [R_x\ R_y\ R_z]^T$ is the distance from the origin of the body frame to the IMU frame, $\omega_b = [\omega_x\ \omega_y\ \omega_z]^T$ is the angular velocity of the body frame and $\alpha_b = [\alpha_x\ \alpha_y\ \alpha_z]^T$ is the angular acceleration of the body frame. The relationship between the various accelerations are

$$a_b + a_R + a_T + a_g = K_a \cdot a_I \quad (3)$$

$$a_I = \widetilde{a_I} - a_{I,n} - a_{I,o} \quad (4)$$

where a_I is the raw acceleration measurement from the IMU, including noise $a_{I,n}$ and bias $a_{I,o}$ in the IMU frame, $K_a \in \mathbb{R}^3$ is a gain and cross correlation matrix, a_b is the translation

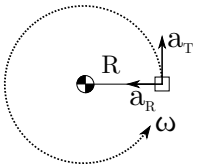

Fig. 3. *Radial and tangential accelerations when IMU is mounted off-center compared to body frame.*

acceleration of the body frame, a_g is the gravity vector in the body frame. Ideally, the matrix K_a is a pure rotational matrix [2] given by the three angles ϕ_I, θ_I, ψ_I. However, if the IMU's coordinate axes X_I, Y_I, Z_I have an axis-to-axis misalignment, or the scaling of at least one of the axes are different than the others K_a will no longer be a proper rotational matrix [5].

The IMU's gyroscopes measure the angular rates ω_I, which are not affected by the location of the IMU relative to the CG, only its orientation given by ϕ_I, θ_I, ψ_I.

$$\omega_b = K_\omega \cdot \omega_I \quad (5)$$

$$\omega_I = \widetilde{\omega_I} - \omega_{I,o} - \omega_{I,n} \quad (6)$$

where K_ω is the gain and cross correlation matrix ω_b is the angular rate of the body frame, $\omega_{I,n}$ is the noise of the gyroscope, $\omega_{I,o}$ is the gyroscope bias and $\widetilde{\omega_I}$ is the gyroscope measurement including noise and bias.

B. Stewart Platform

A Stewart Platform shown in Fig. 4 is used to calibrate the IMU. The Stewart Platform has six degrees of freedom and can manipulate rotations and translations. The Stewart Platform is also able to set the center of rotation to a specific location. This makes it possible to mount any UAV on top of it, and to align the Stewart Platforms center of rotation with the UAV's CG. Different types of motion profiles with different frequencies and amplitudes were generated. Six degrees of freedom data were recorded for positions, velocities and accelerations in the fixed world frame. These measurements were transformed to the UAV body frame.

Fig. 4. *Stewart Platform used for IMU calibration experiments.*

C. Laser Tracker

To verify the motion of the Stewart platform a FARO laser tracker as shown in Fig. 5 was used to verify its position. In the verification it was found that the accuracy of the internal measurements of the Stewart Platform were comparable with the laser tracker, typically in the range 10-30 μm. Hence, in the experimental results presented in this paper, only the internal measurements from the Stewart Platform were used.

Fig. 5. *FARO laser tracker used to verify the internal measurements of the Stewart Platform.*

III. CALIBRATION CONCEPT

The UAV is mounted on top of the Stewart Platform with aligned axes and CG, shown in FIG 6.

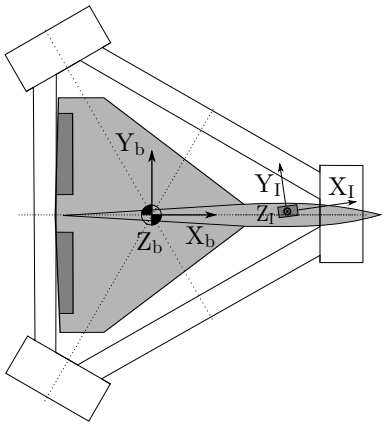

Fig. 6. *UAV mounted for calibration*

The calibration consists of three different stages.

A) Remove offsets
B) Calculate scaling and correlation matrices
C) Find the location of the inertial measurement units R_x, R_y and R_z positions

A. Offset Calibration

The gyroscope bias are removed by calculating the average output over a period of time, with the gyroscope in a fixed position. The bias is subtracted from the gyroscope as given by (6). Acceleration bias can be calculated by taking two measurements, where one measurement is taken while the sensor is turned 180 degrees compared to the first measurement, this is however not done in this paper.

B. Scaling and Correlation

In order to calculate the two matrices K_a and K_ω, two separate tests had to be done, where the first test calculates K_a and the second calculates K_ω. The series of measurement data were synchronized in time for both the Stewart Platform and the IMU. The motion to calculate K_a consists of rapid translative motions, combined with a slow rotation around every body axis. The translative motions manipulate the accelerometer directly, while the slow rotations makes the gravity affect each axis of the IMU dynamically. The Stewart Platform has a force limit for each actuator which in turn limits the maximum acceleration. Adding the rotating gravity vector relative to the IMU increases the acceleration measured by the accelerometer and hence the the signal-noise ratio. The rotation frequency of 0.01Hz is very low, as a result a_g in eq.(3) dominates a_R and a_T which can be neglected from the equations.

The motion to calculate K_ω was a pure rotation about the body axes X_b, Y_b, Z_b. The amplitude and frequencies were higher than for K_a resulting in larger rotational velocities. Typical frequencies generated by the Stewart Platform were in the range 0.6-0.7 Hz with an amplitude of 10 degrees.

For both the accelerometer and gyroscope the problem can be written on the form:

$$\Omega_b = K \cdot \Omega_I \tag{7}$$

where Ω_b is a $3 \times n$ matrix with the true datasets from the Stewart Platform, $K \in \mathbb{R}^3$ is the correlation and scaling matrix, Ω_I is a $3 \times n$ matrix with the measured data, either acceleration or rotational velocity, from the IMU and n is the number of measurement samples. The problem is to find the best fit for K over the data sets. As noted in [9], several optimization criteria have been used for estimation purposes over the years, but the most important ones, at least in the sense of having had the most applications, are criteria that are based on quadratic cost functions. The most common among these is the linear least-squares criterion.

Each column in (7) represents a data set, X, Y and Z respectively. The objective of the least-squares problem is to determine the vectors in the column space of K that is closest to the vectors in Ω_b in the least-squares sense.

$$\min_{\Omega_I} ||\Omega_b - K\Omega_I||^2 \tag{8}$$

The final solution to the problem is:

$$\begin{aligned} \Omega_b &= K \cdot \Omega_I \\ \Omega_b \cdot \Omega_I^T &= K \cdot \Omega_I \cdot \Omega_I^T \\ K &= \Omega_b \cdot \Omega_I^T \cdot (\Omega_I \cdot \Omega_I^T)^{-1} \\ K &= \Omega_b \Omega_I^+ \end{aligned} \tag{9}$$

where Ω_I^+ is the Moore-Penrose pseudoinverse and will exist and be unique for any Ω_I [4]. This approach (9) is used in order to calculate the two matrices K_a and K_ω.

C. Location of the inertial measurement unit

The last step is to calibrate the position $R = [R_x\ R_y\ R_z]^T$ of the IMU relative to CG. The distance vector R can be calculated from (1) and (2) by rotating around one axis at a time. Rotating around the body frame x-axis yields:

$$\begin{aligned} a_{b,x} &= 0 \\ a_{b,y} &= -\alpha_{b,x} \cdot R_z - \omega_{b,x}^2 \cdot R_y \\ a_{b,z} &= \alpha_{b,x} \cdot R_y - \omega_{b,x}^2 \cdot R_z \end{aligned}$$

and in matrix form:

$$\begin{bmatrix} a_{b,x} \\ a_{b,y} \\ a_{b,z} \end{bmatrix} = \begin{bmatrix} 0 & 0 \\ -R_z & -R_y \\ R_y & -R_z \end{bmatrix} \cdot \begin{bmatrix} \alpha_{b,x} \\ \omega_{b,x}^2 \end{bmatrix} \tag{10}$$

Solving the equations using the approach from eq.(9) resolves two sets of R_y and R_z, because of the structure of the matrix in eq.(10). Limitations of the Stewart Platform results in a very low value of ω^2 compared to α. This makes the estimates of R_y, R_z which are multiplied with the angular acceleration α_x more trustworthy than the same estimates multiplied with the angular velocity ω_x^2. Because of this result the estimates multiplied with the accelerations are kept as the final calibrations. The resulting equations are:

$$\begin{bmatrix} a_{b,x} \\ a_{b,y} \\ a_{b,z} \end{bmatrix} = \begin{bmatrix} 0 \\ -R_z \\ R_y \end{bmatrix} \cdot \alpha_{b,x} \tag{11}$$

Doing this for each of the three axes results in two calculations for each distance. If the two datasets are identical it is a verification of the test method of the IMU.

IV. EXPERIMENTS

A. Remove bias

The first experiment was to remove the gyro offsets. The offset was calculated as the mean value of 10.000 samples:

$$\omega_{I,o} = \begin{bmatrix} -0.0043 \\ 0.0010 \\ 0.0048 \end{bmatrix} \frac{rad}{sec} \tag{12}$$

B. Scaling and correlation

The scaling and cross correlation matrix of the gyroscopes were then calculated. For the method to be able to separate the data the test has to be as complex as possible. Running a sine function at each body axis with a the same frequency, only phase shifted, will not result in a correct calculation of the K-matrix. For instance doing a test with the same frequency for each body axis only with a $\frac{\pi}{2}$ rad phase on the y-axis will not result in correct calculations. Assuming that the IMU reference frame is perfectly aligned with the body frame, and the IMU is perfectly scaled and has perpendicular axes, the method will not be able to separate the rotation around the x and the y-axis. The resultant K-matrix will be

$$\begin{bmatrix} \omega_{b,x} \\ \omega_{b,y} \\ \omega_{b,z} \end{bmatrix} = \begin{bmatrix} 0.5 & 0.5 & 0 \\ 0.5 & 0.5 & 0 \\ 0 & 0 & 1 \end{bmatrix} \cdot \begin{bmatrix} \omega_{I,x} \\ \omega_{I,y} \\ \omega_{I,z} \end{bmatrix}$$

and if the phase difference of $\omega_{b,x}$ and $\omega_{b,y}$ is π rad, the rotation of the X_b- and Y_b-axis will be opposite and a negative sign will occur in the correlation matrix:

$$\begin{bmatrix} \omega_{b,x} \\ \omega_{b,y} \\ \omega_{b,z} \end{bmatrix} = \begin{bmatrix} 0.5 & -0.5 & 0 \\ -0.5 & 0.5 & 0 \\ 0 & 0 & 1 \end{bmatrix} \cdot \begin{bmatrix} \omega_{I,x} \\ \omega_{I,y} \\ \omega_{I,z} \end{bmatrix}$$

In order to overcome this, a sine-function with different frequencies were used.

$$\begin{aligned} \omega_{b,x} &= A \sin(2\pi f_x\, t) \\ \omega_{b,y} &= A \sin(2\pi f_y\, t) \\ \omega_{b,z} &= A \sin(2\pi f_z\, t) \end{aligned}$$

where the amplitude $A = 4$ degrees and the frequency $f_x = 0.6$ Hz, $f_y = 0.65$ Hz, $f_z = 0.7$ Hz. Using the approach from (9) with a number of 10.000 sampled datasets from the Stewart Platform and the IMU gives:

$$K_\omega = \begin{bmatrix} 0.95 & 0.29 & 0.01 \\ -0.29 & 0.95 & 0.01 \\ -0.01 & -0.01 & 1.00 \end{bmatrix} \tag{13}$$

The same approach was followed for the accelerometer. The resultant K_a matrix is:

$$K_a = \begin{bmatrix} 0.97 & 0.27 & 0.02 \\ -0.30 & 0.97 & -0.01 \\ 0.01 & 0.01 & 1.00 \end{bmatrix} \tag{14}$$

A result of the measured angular velocity w_I multiplied with the correction matrix K_ω is shown in Fig. 7, and for the accelerometer in Fig. 8. The figures are for a different dataset than for the calculation of K_ω and K_a.

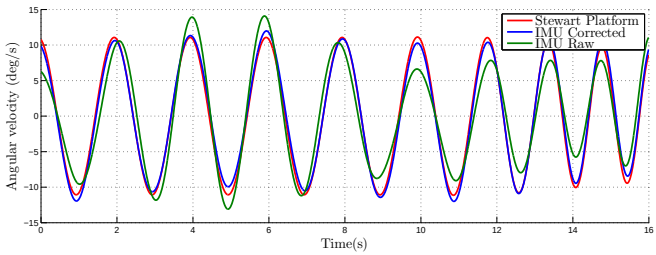

Fig. 7. *Gyroscope scaling and correction for $\omega_{b,x}$, $\omega_{I,x}$ corrected and $\omega_{I,x}$ raw.*

The IMU's orientation was measured to be:

$$\begin{aligned} \phi_I &= 0\ deg \\ \theta_I &= 0\ deg \\ \psi_I &= 17\ deg \end{aligned}$$

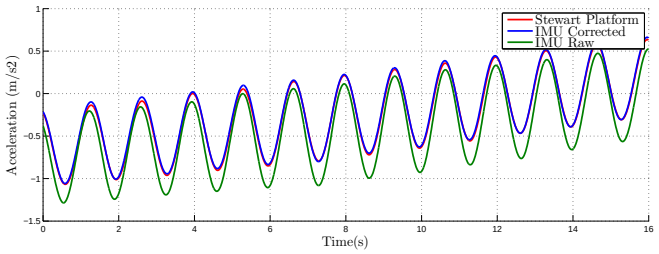

Fig. 8. *Accelerometer scaling and correction for $a_{b,x}$, $a_{I,x}$ corrected and $a_{I,x}$ raw.*

Assuming the IMU is ideal (scaling is perfect and the axis-to-axis misalignment is zero) then the resultant K-matrices would be a rotation matrix. A XYZ rotation matrix is defined as [12] and [3]:

$$C = \begin{bmatrix} c\theta_I c\psi_I & s\phi_I s\theta_I c\psi_I - c\phi_I s\psi_I & c\phi_I s\theta_I c\psi_I + s\phi_I s\psi_I \\ c\theta_I s\psi_I & s\phi_I s\theta_I s\psi_I + c\phi_I c\psi_I & c\phi_I s\theta_I s\psi_I - s\phi_I c\psi_I \\ -s\theta_I & s\phi c\theta_I & c\phi_I c\theta_I \end{bmatrix} \tag{15}$$

where C is the rotation matrix from the IMU frame to the body frame, c is the cosine function and s is the sine function. Inserting the measured values in the rotation matrix C yields:

$$C = \begin{bmatrix} 0.96 & -0.29 & 0 \\ 0.29 & 0.96 & 0 \\ 0 & 0 & 1 \end{bmatrix} \tag{16}$$

The measured correction matrices are very close to the ideal one, K_ω is the one which is closest. There are many reasons why K_a is a bit off. One reason could be the scaling, and correlation are different for the accelerometer than for the gyroscope. The ADIS16400 is however a high-end IMU with less than 0.2 degrees misalignment of the internal axes. Another issue could be that the accelerometer has a range of ± 18 g, which makes it impossible for the Stewart Platform to use the whole range. The range of the excited acceleration to the IMU compared to the accelerometer noise is also significantly less than for the gyroscopes.

C. Location of the inertial measurement unit

The result of K_a from (14) was used in order to correct the acceleration measurement when calculating the position of the IMU, R, as in (3). The Stewart Platform was run in three steps, where each step was a rotation around the X_b, Y_b, Z_b axis respectively. The amplitude was 5 degrees and with a frequency of 0.7 Hz. The same approach as for the calculation of K_a and K_ω (9) was used to calculate R. According to (11) two sets of each distance will be calculated. The results are displayed in table I:

The IMU's position was measured in meters to be:

$$R = \begin{bmatrix} 0.365(m) \\ -0.235(m) \\ 0.230(m) \end{bmatrix}$$

TABLE I

RESULT OF CALCULATION OF THE DISTANCES R_x, R_y AND R_z, RESULTS ARE IN METERS (M)

Rotation axis	R_x	R_y	R_z
ω_x :	–	-0.237	0.227
ω_y :	0.362	–	0.233
ω_Z :	0.362	-0.239	–

A comparison of the measured values with the calculated ones, shows that the error range is less than 5 mm.

D. Full system test

A full system test was done in order to verify the calculated correction matrices and distances. K_a, K_ω and the calculated distances R_x, R_y, R_z was used according to (3) with rotation about the three body axes X_b, Y_b, Z_b:

$$\omega_{IC} = K_\omega \cdot \omega_I \tag{17}$$

$$a_b + a_g = K_a \cdot a_I - \omega_{IC} \times (\omega_{IC} \times R) - \dot{\omega_{IC}} \times R \tag{18}$$

where ω_{IC} is the corrected rotational velocity measured by the gyroscope and $\dot{\omega_{IC}}$ is the time derivative of the rotational velocity.

The results are shown in Fig. 9

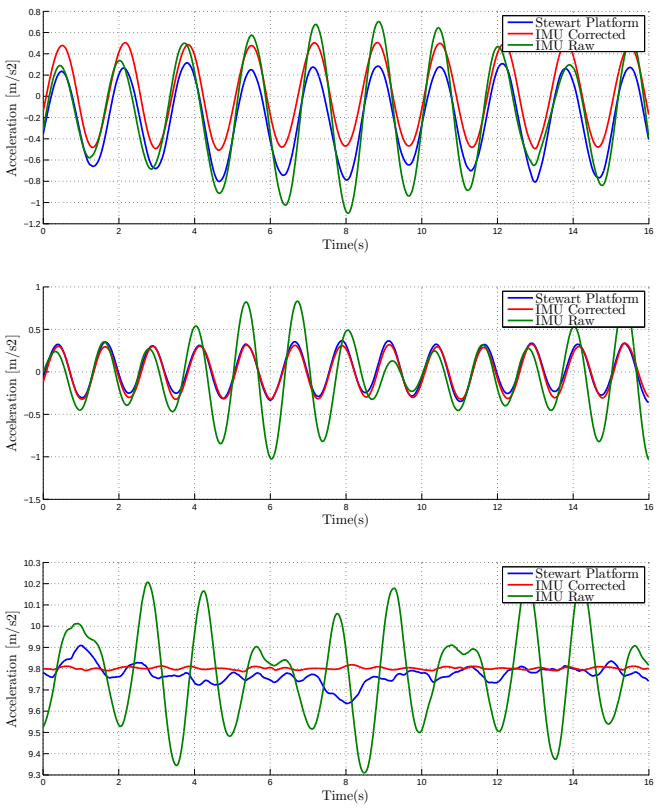

Fig. 9. Comparison of the acceleration from the Stewart Platform, the corrected acceleration from the IMU and the non-corrected acceleration from IMU, for a_x, a_y and a_z respectively

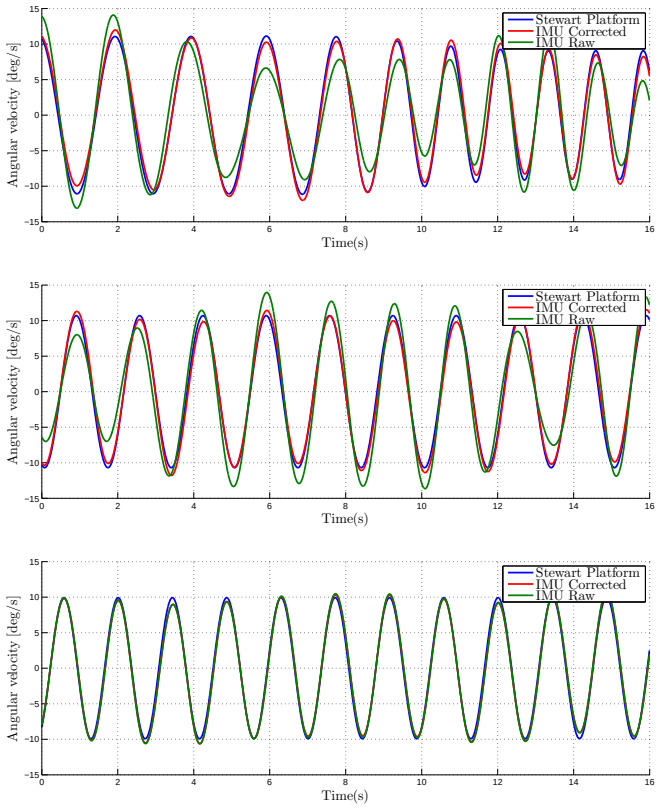

Fig. 10. Comparison of the rotational velocity from the Stewart Platform, the corrected rotational velocity from the IMU and the non-corrected rotation velocity from IMU, for ω_x, ω_y and ω_z respectively

The root-mean-square (RMS) of the signals is a verification of how good the estimates are as a mean. The RMS defined below is an overall verification of how close the estimated values are to the true signal. The signal from the Stewart Platform is subtracted from the signals from the IMU. The difference is squared so that the negative signals will be positive. The RMS is defined as:

$$RMS = \sqrt{\frac{1}{n}\sum_{i=1}^{n}(x_I - x_J)^2} \tag{19}$$

where n is the number of samples, x_I is the IMU sampling data and x_J is the Stewart Platform sampling data.

TABLE II

RESULTS OF THE RMS CALCULATION FOR THE CORRECTED DATA SET

a_x	0.264	
a_y	0.058	(m/s^2)
a_z	0.177	
ω_x	0.0123	
ω_y	0.0123	$(^o/s)$
ω_z	0.0107	

V. CONCLUSIONS

This paper has demonstrated a stepwise calibration method for an ADIS16400 IMU mounted on a UAV by using a 6-DOF Hexapod motion generator. Separate motion profiles were used to calibrate different types of IMU parameters, such as offsets, scaling, axis-to-axis misalignment as well as translational and rotational offsets relative to the body frame of the UAV. The experimental results show an achieved accuracy of typically 0.1-0.3 m/s^2 for the linear accelerations and typically 0.01-0.015 rad/s for the rotational velocities during a test motion profile with motion frequencies of 0-1Hz, 5^o angular range and 0.1m positional range. The test motion profile was independent from the motion profiles used for calibration. The achieved accuracies correspond to 0.17% and 0.25% of the ADIS16400 measurement range for linear acceleration and rotational velocity, respectively. The work presented in this paper demonstrates that a 6-DOF hexapod is well suited for calibration of an IMU when mounted on a UAV.

REFERENCES

[1] M.D Ardema. *Newton-Euler Dynamics*. Springer, 2005.

[2] R.W Beard and T.W McLain. *Small Unmanned Aircraft Theory and Practice*. Princeton University Press, 2012.

[3] G. Genta. *Introduction to the Mechanics of Space Robots*. Springer, 2012.

[4] G.H Golub and C.F Van Loan. *Matrix Computations, 3rd ed.* The Johns Hopkins University Press, 1996.

[5] M.S. Greval and A.P Andrews. *Kalman Filtering Theory and Practice using MATLAB*. Wiley-IEEE Press, 2008.

[6] J.C. Hung and H.V. White. Self-alignment techniques for inertial measurement units. *Aerospace and Electronic Systems, IEEE Transactions on*, AES-11(6):1232 –1247, nov. 1975.

[7] Daniel Mellinger, Quentin Lindsey, Michael Shomin, and Vijay Kumar. Design, modeling, estimation and control for aerial grasping and manipulation. In *Intelligent Robots and Systems (IROS), 2011 IEEE/RSJ International Conference on*, pages 2668 –2673, sept. 2011.

[8] L. Sahawneh and M.A. Jarrah. Development and calibration of low cost mems imu for uav applications. In *Mechatronics and Its Applications, 2008. ISMA 2008. 5th International Symposium on*, pages 1 –9, may 2008.

[9] A.H Sayed. *Digital Signal Processing Fundamentals*. CRC Press, 2012.

[10] A.A Shabana. *Dynamics of Multibody Systems , 2nd ed.* Cambridge Unversity Press, 1998.

[11] K.J. Shortelle, W.R. Graham, and C. Rabourn. F-16 flight tests of a rapid transfer alignment procedure. In *Position Location and Navigation Symposium, IEEE 1998*, pages 379 –386, apr 1998.

[12] B. Siciliano, L. Sciavicco, L. Villani, and G. Oriolo. *Robotics Modelling, Planning and Control*. Springer, 2011.